Vol.8 Issue 2 April 2025

Journal of Networking and Communication Systems

Received 7 April, Revised 13 April, Accepted 29 April

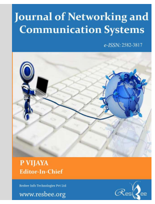

Channel Estimation in Massive MIMO-NOMA with Pilot Contamination Using Deep Kronecker Network

R. Creesy
Department of CSE (AIML)
S.A.Engineering College,
Thiruverkadu, Chennai-77. Tamil Nadu, India.
creesy@saec.ac.in

Abstract: Nowadays, Massive Multiple-Input Multiple-Output (MIMO) is becoming the primary technology in 5th generation (5G) networks, whereas Non-Orthogonal Multiple Access (NOMA) utilizes multiple users to superimpose signals for sharing data. The MIMO-NOMA concept is considered an appealing technology that helps to increase the spectral efficiency and capacity of the reinforcement system during communication. This combination of MIMO and NOMA is seen as a key enabler for addressing the growing demand for high-speed, low-latency communication in modern wireless systems. Generally, MIMO-NOMA systems are used to provide large connectivity by utilizing machine-type devices for the transmission of the same frequency resources. Meanwhile, the channel estimation procedure followed is affected by decoding different user signals. In this article, the Fractional Starfish Optimization Algorithm+Deep Kronecker Network (FSFOA+DKN) is designed to estimate channels in MIMO-NOMA, considering pilot contamination. Initially, the pilot-aided optimal location is identified by the Fractional Starfish Optimization Algorithm (FSFOA) at the transmitter, and the channel prediction is effectuated using the Deep Kronecker Network (DKN) at the receiver. This hybrid approach effectively combines the strengths of metaheuristic optimization and deep learning to improve estimation accuracy. Moreover, Quadrature Amplitude Modulation (QAM) mapping is used for increasing the bandwidth utilization and transmission efficiency. Moreover, the supremacy of FSFOA+DKN in channel estimation is validated, where the FSFOA+DKN attained a Bit Error Rate (BER) of 4.92 x10-7 and Normalized Mean Square Error (MSE) of 0.02.

Keywords: Pilot Contamination, Non-Orthogonal Multiple Access, Deep Learning, Optimization, Massive Multiple-Input Multiple-Output

Nomenclature

Abbreviation	Description
MIMO	Multiple-Input Multiple-Output
NOMA	Non-Orthogonal Multiple Access
DL	Deep Learning
DKN	Deep Kronecker Network
BS	Base Station
UE	User Equipment
CSI	Channel State Information
PC	Pilot Contamination
URLLC	Ultra-Reliable and Low-Latency Communication
SNR	Signal-to-Noise Ratio

1. Introduction

NOMA is an optimum method used to increase the spectrum efficiency of 5G networks, which also captures huge interest among industry and academia [4]. NOMA is designed based on the idea of multiplexing multiple users over the same orthogonal resource block, like subcarrier and time slot [12]. NOMA helps to reduce the latency of the network and provides massive connectivity abilities. Generally, the NOMA permits numerous User Equipment (UE) to simultaneously transmit and receive signals in similar resources [3]. At the same time, MIMO is a technique used to increase the radio link capacity by utilizing multiple receiving and transmitting antennas. The spatial diversity and multipath propagation of wireless channels are exploited by

MIMO by employing additional antennas at both the receiver and transmitter [4][7]. Usually, the same time-frequency resources are reused by multiple users to distinguish signals concerning the responses of the channel in massive MIMO. Thus, it is more crucial to accurately get the information on the channel state at each base station antenna [8]. The integration of massive MIMO and NOMA is considered a more effective way to handle the necessities of massive connectivity [3]. Moreover, the incorporation of the MIMO technique into NOMA effectively provided solutions to challenges, such as high reliability, low latency, and massive connectivity, to further increase the performance by providing an extra degree of freedom to the system. Also, the MIMO-NOMA combination helps to reduce the latency as well as increase the spectral efficiency of communication networks [4]. This combination has become a key enabler for future wireless systems, especially in scenarios requiring ultra-reliable and low-latency communication (URLLC). The increased demands for high-quality service and efficient network management make the combination of MIMO and NOMA a key area of research for next-generation wireless communication.

At present, channel estimation is the most commonly investigated technology, which helps to compute the information of transmission channels [2]. In a massive MIMO-NOMA system, channel estimation is a crucial task that helps to scale up multi-user MIMO to increase the energy and spectral efficiency [3]. Meanwhile, the channel estimation technique is not perfect for all scenarios [2]. Also, the estimated channel not only involves desired channels but also comprises user terminal channels that utilize the same pilot signal in other cells. In general, the accuracy of the estimated channel is degraded by the interference and is termed pilot contamination [1]. The pilot contamination mainly influences the channel information state in the channels used at the base station. The channel estimation of the massive MIMO-NOMA system is affected by the linear merging of another channel. This interference leads to poor quality of service and hinders the system's ability to support multiple users efficiently. To mitigate these challenges, novel optimization and machine learning approaches are being explored, offering new avenues for improving channel estimation accuracy. Nowadays, pilot contamination is eliminated by utilizing the pilot reuse series method in an edge user to attain large-scale, comprehensive information during channel estimation. Also, a semi-blind channel estimation method is used in massive MIMO-NOMA systems for reducing the pilot overhead issues by utilizing transmission data statistics to mitigate the developed pilot contamination [3]. Meanwhile, these techniques are not suitable for MIMO-NOMA systems with massive connectivity. Thus, it is important to reuse the pilots in cells to minimize the pilot overhead issues [10][11]. Nowadays, deep learning techniques have gained promising solution that intelligently and effectively overcomes different technical challenges to increase the effectiveness of wireless communication systems. Moreover, various design approaches are considered by deep learning methods developed for different massive MIMO-NOMA systems [6]. Also, the deep learning techniques design channel estimators and pilot signals jointly in a massive MIMO-NOMA system for reducing pilot contaminations [7][9]. The use of deep learning methods presents a significant advantage by dynamically adapting to network conditions, improving the system's robustness against interference, and enhancing its scalability.

This article presents the FSFOA+DKN designed in massive MIMO-NOMA systems for channel estimation. The process is executed in the transmitter as well as receiver phases, where the input data is passed to a demultiplexer for the conversion of the input data into various data streams. After that, the data is transmitted simultaneously to Serial to Parallel (S/P) conversion, and the QAM mapping process is executed to increase bandwidth utilization and data efficiency. After the QAM mapping process, the pilot-aided optimal location is identified by FSFOA, and the data is transmitted to the receiver phase. The channel prediction is executed by DKN based on the signal characteristics, and the QAM demapping is executed. Following this, the Parallel-to-Serial (P/S) conversion of the received signal is performed, and the actual data is finally retrieved by multiplexing. The introduction of FSFOA+DKN into the system allows for a more accurate estimation of the channel state, even in environments with pilot contamination.

The key research contribution is summarized as,

- **Developed FSFOA+DKN to estimate channel in MIMO-NOMA with pilot contamination:** The FSFOA is designed to identify pilot-aided optimal location, and the channel prediction in massive MIMO-NOMA systems is executed using DKN. Here, the FSFOA is developed by integrating Fractional Calculus (FC) and Starfish Optimization Algorithm (SFOA). This hybrid approach leverages the strengths of both fractional calculus for precise optimization and starfish optimization for efficient search mechanisms.

The remaining portion of the article is organized by: the prevailing schemes employed for channel estimation in MIMO-NOMA are presented in section 2. Section 3 portrays the FSFOA+DKN model. Finally, section 4 describes the experimental outcomes and the following analysis, and section 5 depicts the conclusion of the article.

2. Motivation

The MIMO-NOMA systems help to simultaneously support a large number of users by allocating non-orthogonal resources in NOMA and leveraging the huge number of antennas in massive MIMO. Nowadays, various approaches are utilized for channel estimation by minimizing the pilot contamination. Meanwhile, these approaches recorded high error rates for channel estimation and pilot design in massive MIMO-NOMA systems. Hence, a novel framework named FSFOA+DKN is developed for channel estimation. This framework aims to enhance robustness and accuracy while maintaining lower computational overhead in real-time network environments.

2.1. Literature Review

Hirose, H., *et al.* [1] designed the CNN technique for channel estimation in MIMO-NOMA by mitigating various challenges encountered by pilot contamination and channel aging. The CNN model was robust in accurately estimating channels in interference and dynamic-prone frameworks. However, this model was not successful in utilizing the application of advanced deep learning architectures, like recurrent neural networks or transformers, to increase the efficiency of channel estimation. Additionally, the model's performance degraded under rapidly fluctuating network topologies. Chen, S., *et al.* [2] introduced the Spatial Correlation Block Sparse Bayesian Learning (SC-BSBL) algorithm for channel estimation and User Activity Detection (UAD). The SC-BSBL approach effectively minimized the error rates under less computational cost in a grant-free MIMO-NOMA system while mining the block sparsity of signals. However, this approach failed to increase the capacity algorithm by utilizing more intelligent optimization methods. Moreover, it lacked a mechanism for real-time adaptation to variable traffic loads. Gollagi, S.G., *et al.* [3] developed War Strategy Chimp Optimization+Deep Neuro-Fuzzy Network (WSChO+DNFN) for channel estimation by reducing pilot contamination in massive MIMO-NOMA systems. The WSChO+DNFN model was simple and less complicated. Nevertheless, this approach failed to consider time division methods to receive or transmit signals in all directions. It also did not adequately address scalability in high-density user environments. Kanzariya, D., *et al.* [4] established a deep learning-based MIMO NOMA system for estimating the condition of the channel. This model effectively identified the characteristics of the channel and addressed detection issues under low signal error rates. Meanwhile, this model failed to follow instantaneous fading conditions to extend to time-varying fading channel scenarios. Thus, its performance in mobile communication scenarios with frequent handovers remained uncertain. Nguyen, C., *et al.* [5] devised a CNN-Long-Short Term Memory (LSTM) for channel estimation in the Reconfigurable Intelligent Surface (RIS)-NOMA system. The CNN-LSTM model was robust in channel estimation without any energy loss for the prediction of cascaded channels. Meanwhile, this scheme was not successful in the scenario of communication and integrated sensing. Its efficiency was also limited in scenarios requiring low-latency feedback for real-time applications.

2.2. Challenges

The limitations of techniques are enumerated below,

- The CNN model utilized in [1] significantly mitigated the effects of channel aging under less computational time, but the model failed to dynamically adapt the process followed for channel estimation in large dynamic environments. Also, this approach failed to devise adaptive strategies and investigate the impacts of various pilot contamination levels for mitigating the pilot contamination levels.
- Furthermore, the approach lacked generalization capabilities when applied to diverse wireless scenarios.
- The SC-BSBL approach employed in [2] degraded reconstruction performance and recorded poor convergence effects for low Signal-to-Noise Ratio (SNR), and the total number of users is large.
- The WSChO+DNFN model used in [3] minimized the contamination of pilots, but this model failed to detect a single superposed signal with pilot contamination.
- The prevailing techniques used for channel estimation recorded large feedback, high error rates, and large computational power for channel estimation.
- These limitations indicate a pressing need for hybrid models that combine deep learning with intelligent optimization techniques to address multiple performance factors simultaneously.

3. Designed Fractional Starfish Optimization Algorithm+Deep Kronecker Network for channel estimation with pilot contamination

The FSFOA+DKN is developed in this article in massive MIMO-NOMA systems for channel estimation. The process is mainly executed in the transmitter as well as receiver phases. Initially, the input data is passed to a demultiplexer to convert the input data into data streams. Here, the data is further allowed for S/P conversion, and then, the QAM is carried out. After that, the pilot-aided optimal location is determined by FSFOA, where the FSFOA is designed by integrating FC [15] and SFOA [14]. Following this, the data is transmitted to the receiver phase. In the receiver phase, the transmitted data is received, and the channel prediction is executed by DKN [13] based on the signal characteristics. The DKN utilizes Kronecker structure learning to exploit spatial and temporal dependencies for more accurate prediction. Further, the QAM demodulation is performed, the P/S conversion of the received signal is executed, and the actual data is finally retrieved. In Fig. 1, the diagrammatic representation of FSFOA+DKN for channel estimation is displayed.

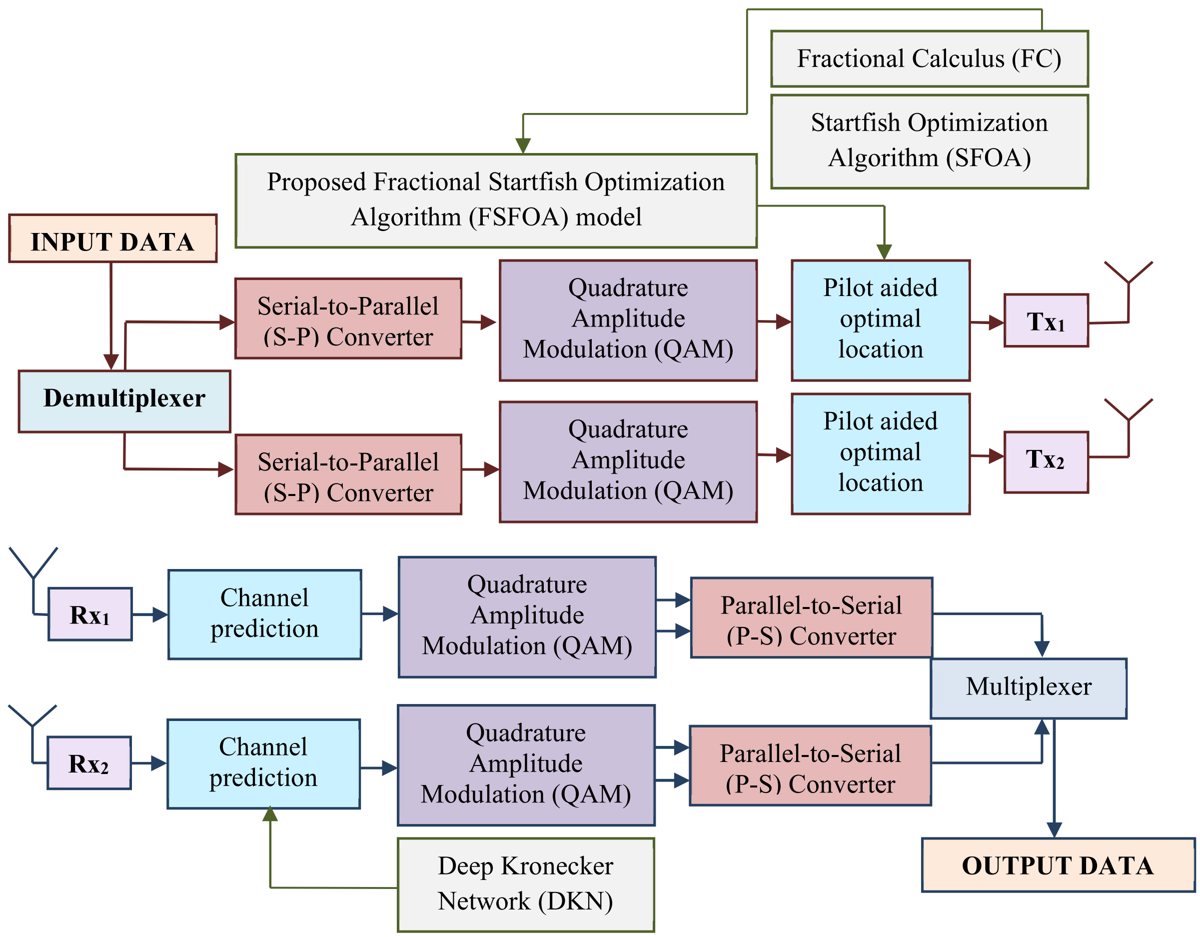

Fig. 1. *Diagrammatic representation of FSFOA+DKN for channel estimation*

3.1. Transmitter Phase

The input data is transmitted to multiple users over the resources with the same time-frequency. Here, the input data is passed to a demultiplexer for the conversion of the input data into various data streams. After that, the data is simultaneously fed into S/P conversion, and the QAM mapping is performed on the transmitted data to enhance the bandwidth utilization and data efficiency, and the FSFOA is used to identify the pilot-aided optimal location. This phase ensures that the data streams are efficiently prepared for parallel transmission while maintaining signal integrity and synchronization across channels.

***a) Demultiplexer*:** A Demultiplexer is a device that helps to split the data into distinct data streams, where the demultiplexing process helps for prioritizing primary data packets and creating multiple outputs. It enables better load balancing across multiple antennas by distributing the data appropriately based on the system's configuration.

***b) S/P converter*:** Single data streams in series are converted into multiple parallel streams in the S/P converter. The S/P converter comprises an interface for serial data input, which enables multiple data streams for various antennas. This parallelism significantly boosts the data rate and supports the high-throughput demands of massive MIMO environments.

***c) QAM mapping*-** The spectral efficiency of the transmitted data is increased by QAM mapping under limited channel bandwidth. Here, the mapping is performed by the combination of two signals, such as the quadrature component and the in-phase component. Typically, the QAM mapping is referred to as the modulation scheme that represents different amplitudes with bits per symbol. It also helps improve signal robustness against noise and distortion by efficiently utilizing the available signal space.

3.1.1 Pilot-aided Optimal Location by Fractional Starfish Optimization Algorithm

The process of enabling accurate channel estimates of all users by executing strategic placement of pilot symbols over space, time, and frequency is performed in the pilot-aided optimal location. It is identified by FSFOA by considering the solution encoding and fitness function. This optimization phase is vital to ensure minimal interference between overlapping pilot signals and enhance system capacity. The process executed during the identification of pilot-aided optimal location is briefly demonstrated as follows,

i) Solution encoding

The solution encoding represents the solutions to Pilot-aided optimal location using FSFOA. In solution encoding, the solutions are initiated randomly by FSFOA to identify the optimal key size. The total number of pilots A is considered for identifying the pilot-aided optimal location for a signal of length P. The encoded solutions guide the FSFOA in navigating the high-dimensional search space to minimize interference and maximize estimation accuracy. Fig. 2 displays the solution encoding performed to select optimal pilots.

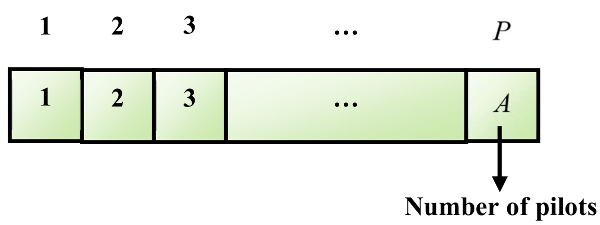

Fig. 2. *Solution encoding*

ii) Fitness function

The minimum fitness is taken into consideration for identifying the pilot-aided optimal location. The fitness function is given as,

$$Fitness\ function = \frac{\gamma}{\lambda} \tag{1}$$

In the expression, the total transferred bits are indicated as λ, and γ the total bit errors. This fitness function acts as a performance metric to minimize bit error rate (BER) during pilot placement.

iii) Designed Fractional Starfish Optimization Algorithm

The pilot-aided optimal location is determined by utilizing the FSFOA model, where the FSFOA is designed by incorporating FC [15] and SFOA [14]. A novel bio-inspired metaheuristic, called SFOA, is designed concerning the natural characteristics of starfish, which include regeneration, preying, and exploration. Among all, exploitation and exploration are the main phases followed in SFOA. Here, the exploitation phase follows a special movement and two-directional strategy to show the regeneration and predatory characteristics of starfish. In the exploration phase, the explorative characteristics are based on the unidimensional and five-dimensional search patterns performed by the starfish. The SFOA converges quickly during exploitation in the search area, which also ensures the search capacity as well as enhances the computational efficiency in the exploration phase. On the other hand, the FC is a subdivision of applied mathematics that uses the Laplace transform to provide solutions to integral and derivative problems. The FC is incorporated with SFOA to enhance the convergence rate of the optimization algorithm. This hybridization improves local optima avoidance and accelerates global convergence under high-dimensional constraints. The modeling of FSFOA is explicated below,

Phase 1: Initialization

The starfish position is randomly generated among the design variables boundaries in the initialization phase, and is designated as,

$$S = \begin{bmatrix} S_{1,1} & S_{1,2} & \cdots & S_{1,c} \\ S_{2,1} & S_{2,2} & \cdots & S_{2,c} \\ \vdots & \vdots & \ddots & \vdots \\ S_{b,1} & S_{b,2} & \cdots & S_{b,c} \end{bmatrix}_{b\times c} \tag{2}$$

Here, the dimension of the design variable is signified as c the population size is represented b , and the starfish position is saved by the matrix given S . During initialization, the position of the starfish is given by,

$$S_{x,y} = M_y + Rand\left(N_y - M_y\right), \quad x = 1,2,3,...,b, \quad y = 1,2,3,...,c \tag{3}$$

In the expression, the lower and upper bound of design variables in y^{th} dimension is signified as M_y , and N_y a random number fixed to [0,1] is indicated as $Rand$, and $S_{x,y}$ is the x^{th} starfish position at y^{th} dimension. This random initialization provides diverse candidate solutions to prevent premature convergence.

Phase 2: Fitness estimation

The expression of the objective function given in equation (1) is utilized for estimating the fitness value of all starfish. Each candidate's fitness is used to guide evolutionary updates in later phases.

Phase 3: Exploration phase

The five arms of the starfish during searching for food are simulated in the exploration phase, where the eyes of the starfish are embedded at the end of the arms. The search space is extensive, and the starfish is required to move all five arms, if the dimension of the optimization issue is higher as compared to 5, i.e $I > 5$. Thus, the knowledge of the best position is required by the arms of the starfish between the search agents. The updated best position of the starfish is articulated as,

$$S_{x,l}\left(d+1\right) = S_{x,l}\left(d\right) + Y_1\left[S_{BEST,l}\left(d\right) - S_{x,l}^{T}\left(d\right)\right]\cos\theta \tag{4}$$

where the five randomly selected dimensions are signified as l the current best position of starfish at d^{th} iteration is signified as $S_{BEST,l}\left(d\right)$, and the current and obtained position of starfish at d^{th} iteration are given as $S_{x,l}\left(d\right)$ and $S_{x,l}\left(d+1\right)$.

The equation (4) becomes,

$$S_{x,l}\left(d+1\right) = S_{x,l}\left(d\right) + Y_1 S_{BEST,l}\left(d\right)\cos\theta - Y_1 S_{x,l}\left(d\right)\cos\theta \tag{5}$$

$$S_{x,l}\left(d+1\right) = S_{x,l}\left(d\right)\left[1 - Y_1\cos\theta\right] + Y_1 S_{BEST,l}\left(d\right)\cos\theta \tag{6}$$

For applying FC, subtract $S_{x,l}\left(d\right)$ both sides of equation (6), and the equation becomes,

$$S_{x,l}\left(d+1\right) - S_{x,l}\left(d\right) = S_{x,l}\left(d\right)\left[1 - Y_1\cos\theta\right] + Y_1 S_{BEST,l}\left(d\right)\cos\theta - S_{x,l}\left(d\right) \tag{7}$$

$$S_{x,l}\left(d+1\right) - S_{x,l}\left(d\right) = Y_1 S_{BEST,l}\left(d\right)\cos\theta - Y_1\cos\theta \tag{8}$$

The FC [15] is integrated with SFOA [14] to enhance the convergence rate of the optimization algorithm. From FC,

$$X^{\delta}\left[S_{x,l}\left(d+1\right) - S_{x,l}\left(d\right)\right] = Y_1 S_{BEST,l}\left(d\right)\cos\theta - Y_1\cos\theta \tag{9}$$

$$\begin{bmatrix} S_{x,l}(d+1)-\delta S_{x,l}(d)-\frac{1}{2}\delta S_{x,l}(d-1)- \\ \frac{1}{6}(1-\delta)S_{x,l}(d-2)-\frac{1}{24}\delta(1-\delta)(2-\delta)S_{x,l}(d-3) \end{bmatrix} = Y_1 S_{BEST,l}(d)\cos\theta - Y_1\cos\theta \tag{10}$$

Thus, the updated final expression of FSFOA is given by,

$$\begin{aligned} S_{x,l}(d+1) = Y_1 S_{BEST,l}(d)\cos\theta - Y_1\cos\theta + \delta S_{x,l}(d) + \frac{1}{2}\delta S_{x,l}(d-1) + \\ \frac{1}{6}(1-\delta)S_{x,l}(d-2) + \frac{1}{24}\delta(1-\delta)(2-\delta)S_{x,l}(d-3) \end{aligned} \tag{11}$$

Here, δ stipulates the order of the derivative. If the dimension of the optimization issue is not higher as compared to 5, i.e $I \le 5$, then the position of the starfish is updated by unidimensional search patterns. Under such conditions, the starfish uses only one arm to find a food source by considering the location information. Thus, the modified starfish position is given by,

$$S_{x,k}(d+1) = ZS_{x,l}(d) + F_1\left[S_{m_1,l}(d) - S_{x,l}^T(d)\right] + F_2\left[S_{m_2,l}(d) - S_{x,l}^T(d)\right] \tag{12}$$

Here, the two random numbers among [-1,1] are represented as F_1 and F_2, the dimensional positions among two randomly selected starfish are symbolized as $S_{m_2,l}(d)$ and $S_{m_1,l}(d)$, and the energy of the starfish is denoted by Z. This adaptation ensures that even low-dimensional problems are effectively explored using minimal search complexity.

Phase 4: Exploitation phase

During exploitation, the regeneration and predatory characteristics of starfish are considered. At first, the five distances among the other starfish and the best location are calculated, and the position of each starfish is selected randomly by using the two-directional search strategies. Thus, the predatory characteristics of the starfish are expressed as,

$$S_x(d+1) = S_x(d) + g_1\kappa_1 + g_2\kappa_2 \tag{13}$$

Here, κ_1 and κ_2 are the random number among [0,1], the randomly selected distance is represented as g_1 and g_2. Further, the last starfish in the population is considered to implement SFOA in the regeneration phase. Hence, the modified rule of starfish in the regeneration phase is expressed as,

$$S_x(d+1) = \exp(-d \times T/d_{\max})S_x(d) \tag{14}$$

where the population size is indicated as T, and the maximum iteration is represented as $d_{\max}$. These phases improve the solution refinement process by exploiting localized information around the best candidates.

Phase 5: Re-estimation of fitness

Equation (1) is used to identify the best candidate solution, where the candidate solution is replaced if any solution is identified as superior as compared to the present candidate solution. This dynamic re-evaluation helps maintain solution quality and adapt to ongoing optimization states.

Phase 6: Termination

The steps followed in FSFOA are repeated continuously till attaining the best candidate solution is attained. Once convergence is achieved or the iteration limit is reached, the final pilot placement is determined.

3.2. Receiver Phase

The actual data is retrieved in the receiver phase by separating the superimposed signals and decoding each transmitted signal individually from the transmitter phase. The channel is predicted using DKN, considering the characteristics of the received signal in the receiver phase. After that, the QAM demapping of the predicted channel is performed, the P/S conversion of the received signal is executed, and the actual data is finally retrieved. This phase is critical for signal recovery and directly affects the end-to-end bit error rate. The process executed in the receiver phase is delineated herewith,

3.2.1. Channel prediction using Deep Kronecker Network

The DKN model [13] is employed for channel prediction, where the DKN is a type of CNN, specifically a Fully Connected Network (FCN), that is designed concerning the Kronecker product structure. The DKN is embedded in a generalized linear model and comprises no overlap convolutions. The DKN is more interpretable and helps to perform both discrete and continuous responses, which also connects the tensor regression framework to significantly minimize the dimension, thereby performing the channel prediction task effectively. Its compact structure ensures reduced complexity while preserving accuracy in high-dimensional input-output mappings.

Let us consider that there are H samples with a data matrix $G_a \in R^{x \times y}$ and a scalar response E_i, and the scalar response E_i is attained by a generalized linear model, which is given by,

$$E_i \left| G_a \sim J\left(E_i \left| G_a\right.\right) = \alpha\left(E_i\right) \exp\left[E_i \langle G_a, B\rangle - \beta\left(\langle G_a, B\rangle\right)\right]\right. \tag{15}$$

In the expression, the expected unknown coefficient matrix is denoted by $B \in \Re^{x \times y}$, and the known univariate functions are given by $\alpha(.)$ and $\beta(.)$. In DKN, a link function $\rho(.)$ is expressed by,

$$\rho\left(\mathrm{E}\left(E_i\right)\right) = \langle G_a, B\rangle \tag{16}$$

Further, the decomposition of the rank-K Kronecker product is executed by $Q(\geq 2)$ factors, and is given by,

$$B = \sum_{p=1}^{I} W_g^p \otimes W_{g-1}^p \otimes \ldots \otimes W_1^p \tag{17}$$

Here, the size of the W_u^p are not assumed, and the Kronecker factors are given as I, $W_u^p \in \Re^{x_u \times y_u}$, $u = 1, 2, 3, \ldots, Q$, and $p = 1, 2, 3, \ldots, I$, K representing rank, and W is the factor number. However, the Kronecker factors are required to satisfy $x = \prod_{u=1}^{Q} x_u \quad y = \prod_{u=1}^{Q} y_u$ due to the properties of the Kronecker product. Hence, the Kronecker product property for any matrices $W_{u'}, \ldots, W_{u''}$ that satisfy the condition $u' \geq u''$ is articulated as,

$$W_u \otimes W_{u'-1} \otimes \ldots \otimes W_{u''} = \bigotimes_{u=u'}^{u''} W_C \tag{18}$$

In the expression, the expression of decomposition is given by $\sum_{p=1}^{I} \otimes_{u=g}^{1} L_u^p$, where the DKN output is designated as C_P, where the architecture design of DKN is given in Fig. 3. This structural decomposition allows the DKN to effectively capture multiscale dependencies in the received signal.

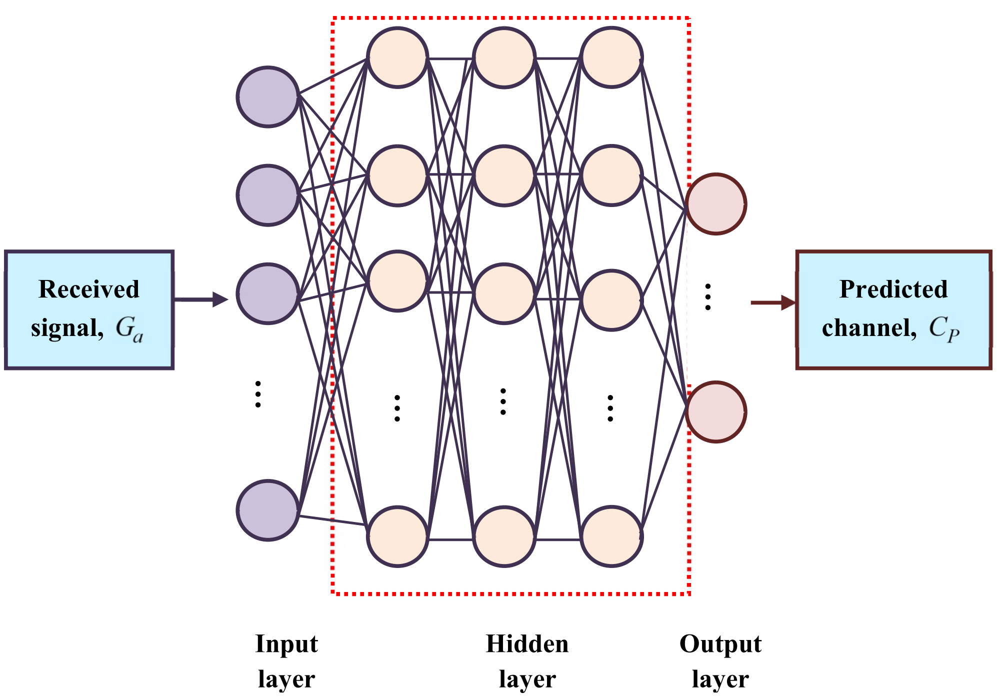

Fig. 3. *Structural design of DKN*

Further, the process carried out during the retrieval of actual data by performing the QAM demapping process, conversion of P/S, as well as multiplexing, is detailed as follows. These processes collectively restore the original bitstream from the received modulated signals, ensuring end-to-end data integrity.

i) QAM demapping: The process of transforming the complex QAM symbols received at the receiver back into corresponding bit sequences is performed in QAM demapping. This step is critical for converting the modulation symbols into digital data that can be decoded and interpreted.

ii) P/S converter: The signals received from multiple antennas/parallel ports are converted into a serial form in the P/S converter. This transformation prepares the signals for final aggregation and reconstruction of the original transmitted message.

iii) Multiplexing: Multiplexing is used to consolidate multiple data sources obtained from different sources interconnected into a single source. In this process, the multiple data streams are converted into a single stream to retrieve the actual data. The multiplexing process ensures that data integrity is maintained while reducing the overhead of managing multiple streams separately.

4. Results and Discussion

This section conducts the investigations performed to validate the supremacy of FSFOA+DKN during channel estimation in the MIMO-NOMA system using different measures. The performance is evaluated under varying conditions to simulate real-world communication scenarios.

4.1. Experimental Set-Up

The FSFOA+DKN, designed for channel estimation with pilot contamination, is implemented in a Python tool with simulation. The experimental environment includes a controlled simulation setting that models practical transmission parameters.

4.2. Evaluation Indicators

The efficacy of the FSFOA+DKN is estimated by utilizing various indicators, and is detailed as follows, These indicators are chosen to comprehensively assess both accuracy and reliability of channel estimation.

a) BER: The robustness of FSFOA+DKN in channel estimation is determined using BER, where the BER helps to identify the quality of communicated channels. The BER is expressed as,

$$BER = \frac{U}{V} \tag{19}$$

In the expression, the total transmitted bits are symbolized as V , and the total error bits are symbolized as U . A lower BER value indicates higher channel prediction precision and fewer transmission errors.

b) MSE: The Mean Square Error (MSE) is used to identify the accuracy of the channel predicted by DKN, and is given as,

$$MSE = \frac{1}{K}\sum_{g=1}^{K}\left(C_{P_g}^{*} - C_P\right)^2 \tag{20}$$

Here, the predicted DKN output is given by C_P the targeted predicted output of DKN is signified as C_P^*, and K is the total samples utilized for training. MSE offers a direct measure of the model's prediction deviation, making it suitable for training evaluation.

4.3. Comparative Models

To validate the supremacy of FSFOA+DKN, the baseline approaches, such as CNN [1], SC-BSBL [2], WSChO+DNFN [3], and CNN-LSTM [5], are employed in this research for comparison with FSFOA+DKN. These comparative models represent state-of-the-art techniques widely adopted for MIMO-NOMA channel estimation.

4.4. Comparative Assessment

The antenna size is varied 2×2 4×4 , and 16×16 by considering SNR for investigating the efficacy of FSFOA+DKN in channel estimation with pilot contamination. The analyses executed are briefly delineated as follows: Varying the antenna size helps examine the scalability and robustness of the FSFOA+DKN under different spatial configurations.

i) For antenna size 2×2

In Fig. 4, the investigation of FSFOA+DKN concerning SNR for antenna size 2×2 is depicted. At first, the validation of FSFOA+DKN employing normalized MSE considering SNR is delineated in Fig. 4(a). Here, the normalized MSE of 0.01 is attained by FSFOA+DKN for 10dB SNR, and the prevailing schemes attained normalized MSEs of 0.07 by CNN, 0.05 by SC-BSBL, 0.04 by WSChO+DNFN, and 0.03 by CNN-LSTM. Moreover, the analysis of FSFOA+DKN by utilizing BER based on SNR is demonstrated in Fig. 4(b). The FSFOA+DKN attained a BER of $1.23\text{x}10^{-3}$ for 10dB SNR, whereas the BER attained by baseline models, such as CNN is $2.09\text{x}10^{-2}$, SC-BSBL is $1.68\ \text{x}10^{-2}$, WSChO+DNFN is $1.40\ \text{x}10^{-3}$, and CNN-LSTM is $4.35\ \text{x}10^{-3}$. This comparative outcome clearly illustrates the superior estimation capability and noise resilience of FSFOA+DKN.

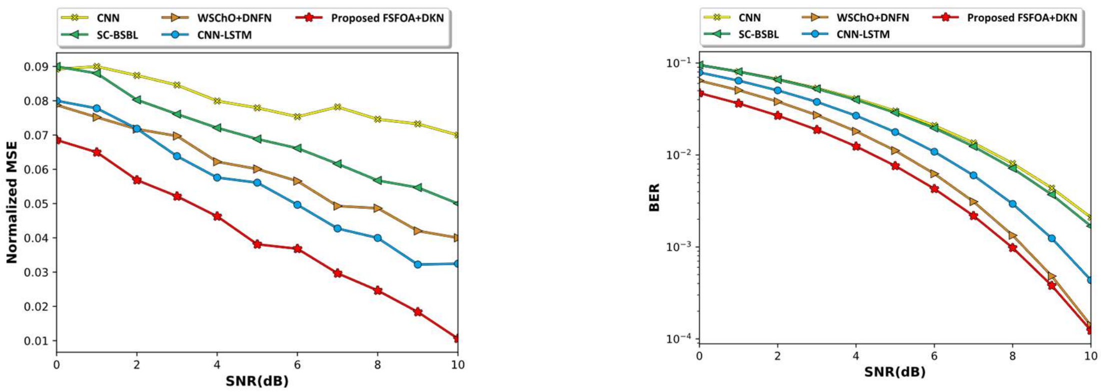

(a) (b)

Fig. 4. *Comparative investigation of FSFOA+DKN by employing (a) Normalized MSE and (b) BER for antenna size* 2×2

ii) For antenna size 4×4

The analysis of FSFOA+DKN for antenna size 4×4 considering SNR is displayed in Fig. 5. The evaluation of FSFOA+DKN based on normalized MSE concerning SNR is depicted in Fig. 5(a). The FSFOA+DKN measured a normalized MSE of 0.02 when the SNR is 10dB, whereas the normalized MSE measured by other prevailing schemes, like CNN, SC-BSBL, WSChO+DNFN, and CNN-LSTM, is 0.08, 0.07, 0.05, and 0.04. This reflects the strong denoising capability of FSFOA+DKN, particularly under moderate SNR conditions. Further, Fig. 5(b) displays the valuation of FSFOA+DKN using BER concerning SNR. The outcomes obtained from the experiment show that the FSFOA+DKN attained a BER of $4.92\ \text{x}10^{-7}$, whereas the BER attained by baseline models, such as CNN is $4.13\ \text{x}10^{-3}$, SC-BSBL is $2.34\ \text{x}10^{-3}$, WSChO+DNFN is $5.67\ \text{x}10^{-6}$, and CNN-LSTM is $2.23\ \text{x}10^{-5}$ for 10dB SNR. This remarkably low BER demonstrates the superior noise suppression and estimation precision achieved by integrating FSFOA with DKN.

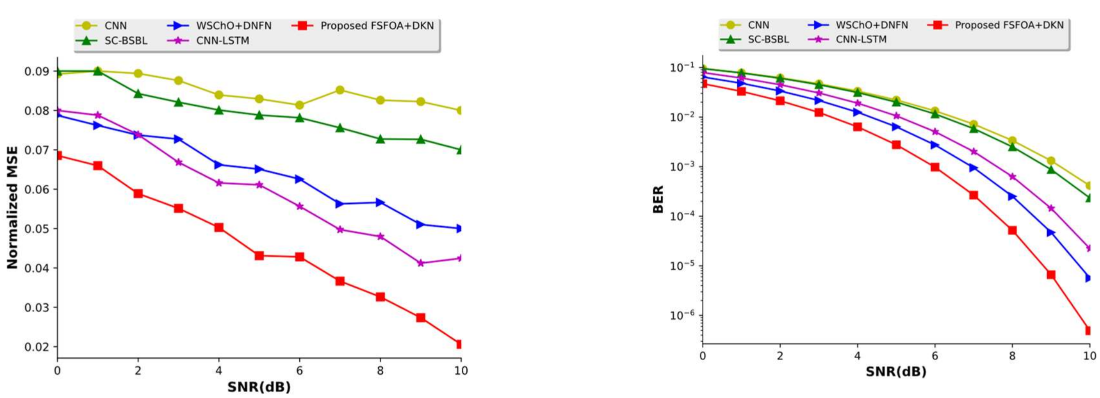

(a) (b)

Fig. 5. *Comparative investigation of FSFOA+DKN by employing (a) Normalized MSE and (b) BER for antenna size* 4×4

iii) For antenna size 16×16

Fig. 6 shows the investigation of FSFOA+DKN for antenna size 16×16 concerning SNR. The validation of FSFOA+DKN utilizing normalized MSE based on SNR is shown in Fig. 5(a). The FSFOA+DKN measured a normalized MSE of 0.03, whereas the normalized MSE measured by other prevailing schemes, like CNN, SC-BSBL, WSChO+DNFN, and CNN-LSTM, is 0.08, 0.07, 0.06, and 0.05 when the SNR is 10 dB. This consistent outperformance of FSFOA+DKN indicates its robustness across varying antenna configurations. In addition to this, the analysis of FSFOA+DKN by utilizing BER considering SNR is shown in Fig. 4(b). As evidenced, the FSFOA+DKN yielded a minimum BER of 1.22 $\times 10^{-6}$ for 10dB SNR, as well as the baseline models, like CNN, SC-BSBL, WSChO+DNFN, and CNN-LSTM, observed BERs of 5.97 $\times 10^{-3}$, 2.72 $\times 10^{-3}$, 2.17 $\times 10^{-5}$, and 8.85 $\times 10^{-5}$. These results confirm the scalability and high performance of FSFOA+DKN even as the number of antennas increases.

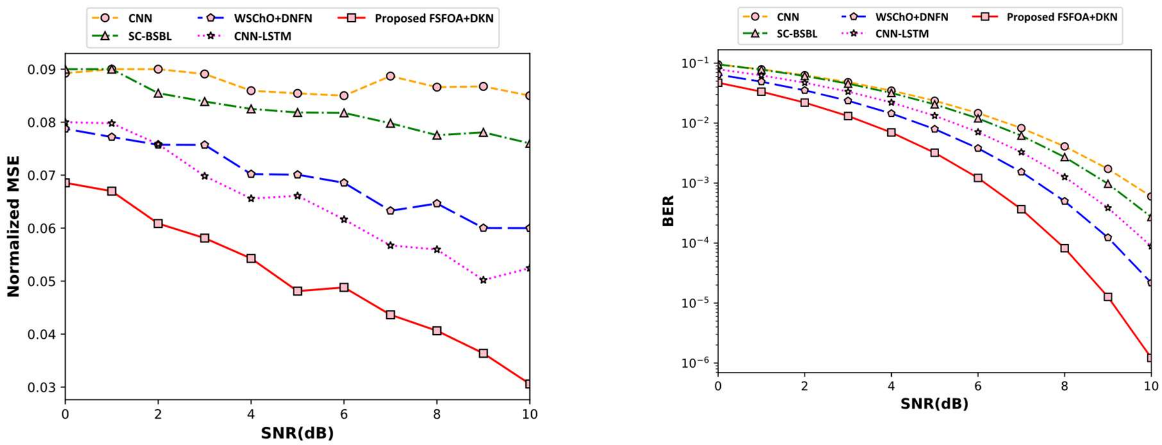

(a) (b)

Fig. 6. *Validation of FSFOA+DKN for antenna size* 16×16 *by employing (a) Normalized MSE and (b) BER*

4.5. Comparative Discussion

The results recorded by FSFOA+DKN, as well as existing schemes employed for comparison by utilizing different measures, are depicted in Table 2. The outcomes obtained from the experiment show that the FSFOA+DKN attained a normalized MSE of 0.02, and a BER of 4.92 $\times 10^{-7}$ for 10dB SNR. Similarly, the normalized MSE measured by existing schemes, like CNN, is 0.08, SC-BSBL is 0.07, WSChO+DNFN is 0.05, and CNN-LSTM is 0.04 for 10dB SNR. Likewise, the existing models like CNN, SC-BSBL, WSChO+DNFN, and CNN-LSTM observed BER of 4.13 $\times 10^{-3}$, 2.34 $\times 10^{-3}$, 5.67 $\times 10^{-6}$, and 2.23 $\times 10^{-5}$. These improvements in both BER and MSE illustrate the effectiveness of combining bio-inspired optimization with deep neural networks for channel estimation. Overall, the experimental results revealed that the FSFOA+DKN yielded superior outcomes than other models employed for comparison. The FSFOA+DKN is more robust in performing channel prediction tasks for efficient and accurate channel state information. This enhanced performance highlights FSFOA+DKN's potential as a practical solution for real-time 5G and beyond wireless systems where low latency and high precision are critical.

Table 2. *Comparative discussion*

Evaluation indicators	Channel estimation techniques				
	CNN	SC-BSBL	WSChO+DNFN	CNN-LSTM	Proposed FSFOA+DKN
For 2×2 antenna size					
BER	2.09×10^{-2}	1.68×10^{-2}	1.40×10^{-3}	4.35×10^{-3}	1.23×10^{-3}
Normalized MSE	0.07	0.05	0.04	0.03	0.01
For 4×4 antenna size					
BER	4.13×10^{-3}	2.34×10^{-3}	5.67×10^{-6}	2.23×10^{-5}	**4.92×10^{-7}**
Normalized MSE	0.08	0.07	0.05	0.04	**0.02**
For 16×16 antenna size					
BER	5.97×10^{-3}	2.72×10^{-3}	2.17×10^{-5}	8.85×10^{-5}	1.22×10^{-6}
Normalized MSE	0.085	0.076	0.06	0.05	0.03

5. Conclusion

This article presents the FSFOA+DKN model developed for channel estimation, where the process is performed in the transmitter and receiver phases. In the transmitter phase, the input data is initially fed into demultiplexing to convert the data into different data streams. Then, the data is simultaneously transmitted to the S/P conversion, and the QAM mapping is performed. After the QAM mapping process, the identification of the pilot-aided optimal location is performed by FSFOA, and the data is transmitted. In the receiver, the channel prediction is performed using DKN based on the signal characteristics once the transmitted data is received by the receiver, and then, the demapping of QAM is executed. Finally, the P/S conversion of the received signal is performed, and the multiplexing is executed to retrieve the actual data. This two-stage approach ensures a structured and efficient processing pipeline that enhances overall channel estimation accuracy. Further, the supremacy of FSFOA+DKN is investigated by comparing it with existing channel estimation schemes, where FSFOA+DKN yielded MSE and BER of 0.02 and 4.92 $x10^{-7}$ respectively. The results demonstrate FSFOA+DKN's potential to serve as a high-performing solution for complex wireless environments, particularly in systems affected by pilot contamination. Future research will be on designing a hybrid deep-learning model for the estimation of channels in MIMO-NOMA.

Compliance With Ethical Standards

Conflicts of interest: Authors declared that they have no conflict of interest.

Human participants: The conducted research follows ethical standards and the authors ensured that they have not conducted any studies with human participants or animals.

References

[1] Hirose, H., Yang, S., Ohtsuki, T., and Bouazizi, M., "Deep Learning-based Channel Estimation to Mitigate Channel Aging in Massive MIMO with Pilot Contamination", IEEE Access, 2024.

[2] Chen, S., Li, H., Zhang, L., Zhou, M. and Li, X., "Block sparse Bayesian learning based joint user activity detection and channel estimation in grant-free MIMO-NOMA", Drones, vol.7, no.1, pp.27, 2022.

[3] Gollagi, S.G., Maheswari, S.S., Sapkale, P.V. and Poojitha, S., "Channel estimation for pilot contamination in massive MIMO-NOMA system", Journal of High-Speed Networks, vol.30, no.3, pp.355-373, 2024.

[4] Kanzariya, D., Trada, P., Kaswala, H. and Shah, H.B., "Deep learning based signal detection and channel estimation for MIMO-NOMA system", Science, vol.1, no.1, pp.23-35, 2022.

[5] Nguyen, C., Hoang, T.M. and Cheema, A.A., "Channel estimation using CNN-LSTM in RIS-NOMA assisted 6G network", IEEE Transactions on Machine Learning in Communications and Networking, vol.1, pp.43-60, 2023.

[6] Guo, J., Chen, T., Jin, S., Li, G.Y., Wang, X. and Hou, X., "Deep learning for joint channel estimation and feedback in massive MIMO systems", Digital Communications and Networks, vol.10, no.1, pp.83-93, 2024.

[7] Kang, J.M., "Deep-learning-based robust channel estimation for MIMO IoT systems", IEEE Internet of Things Journal, vol.11, no.6, pp.9882-9895, 2023.

[8] Li, D.L. and Farhang, A., "Joint channel estimation and equalization in massive MIMO using a single pilot subcarrier", IEEE Wireless Communications Letters, vol.12, no.11, pp.1931-1935, 2023.

[9] Chen, Z., Song, K., Qu, Z., Zhang, Y. and Shang, Y., "Deep-Learning-Based Pilot Optimization for Near-Field Channel Estimation in Ultra-Massive MIMO", Electronics Letters, vol.61, no.1, pp.70227, 2025.

[10] Surendran, J., "Joint channel estimation and signal detection in MIMO-NOMA wireless systems using deep learning", In Proceedings of 2023 IEEE International Conference on Recent Advances in Systems Science and Engineering (RASSE), IEEE, pp. 1-6, 2023.

[11] Apiyo, A. and Izydorczyk, J., "A survey of NOMA-aided cell-free massive MIMO systems", Electronics, vol.13, no.1, pp.231, 2024.

[12] Anu, T.S. and Raveendran, T., "CNN-based channel estimation using NOMA for mmWave massive MIMO system", In Proceedings of 2023 IEEE Statistical Signal Processing Workshop (SSP), IEEE, pp. 349-353, 2023.

[13] Feng, L. and Yang, G., "Deep kronecker network", Biometrika, vol.111, no.2, pp.707-714, 2024.

[14] Zhong, C., Li, G., Meng, Z., Li, H., Yildiz, A.R. and Mirjalili, S., "Starfish optimization algorithm (SFOA): a bio-inspired metaheuristic algorithm for global optimization compared with 100 optimizers", Neural Computing and Applications, vol.37, no.5, pp.3641-3683, 2025.

[15] Bhaladhare, P.R. and Jinwala, D.C., "A clustering approach for the l-diversity model in privacy preserving data mining using fractional calculus-bacterial foraging optimization algorithm", Advances in Computer Engineering, vol.1, p.396529, 2014.